Chemical Engineering Journal 152 (2009) 537–542

Contents lists available at ScienceDirect

Chemical Engineering Journal

journal homepage: www.elsevier.com/locate/cej

Visible light photocatalytic decolourization of C. I. Acid Red 66 by chitosan capped CdS composite nanoparticles

Jiang Ru[a], Zhu Huayue[a,b,*], Li Xiaodong[c], Xiao Ling[b]

[a] Department of Environmental Engineering, Taizhou University, Taizhou 317000, China
[b] College of Resource and Environmental Science, Wuhan University, Wuhan 430072, China
[c] College of Environmental Science and Engineering, Hunan University, Changsha 410082, China

ARTICLE INFO

Article history:
Received 13 January 2009
Received in revised form 21 May 2009
Accepted 21 May 2009

Keywords:
Photocatalytic decolourization
Visible light
C. I. Acid Red 66
Chitosan
Cadmium sulfide

ABSTRACT

Chitosan capped CdS (CS/CdS) composite nanoparticles were prepared by biomimetic synthesis method under mild condition. The CS/CdS composite catalyst was characterized by XRD, SEM, TEM and TGA, which indicated the successful formation of nanosized hexagonal phase of CdS on chitosan. Visible light photocatalytic decolourization of C. I. Acid Red 66 (AR 66) was carried out by employing this innovative composite catalyst. The effects of catalyst amount, initial dye concentration and initial pH of solution on decolourization were investigated. The kinetics of photocatalytic decolourization was found to follow a pseudo-first-order according to Langmiur–Hinshelwood (L–H) model. UV–vis spectra were analyzed to prove that AR 66 dye can be decolourized effectively by chitosan capped CdS composite nanoparticles under visible light irradiation. In addition, the recycle and reuse of the catalyst were examined, and the results showed that dye decolourization efficiency was still about 80.1% after 60 min of reaction time when the catalyst was used for 5 times.

1. Introduction

Textile industry discharges large amount of coloured dye wastewater which is toxic and nonbiodegradable in most cases [1]. Apart from the aesthetic problems created when coloured effluents reach the natural water runoff, dyes strongly absorb sunlight, impending photosynthetic activity of aquatic plants and seriously threatening the whole ecosystem [2]. The decolourization of dyes effluents has always been an attractive and challenging topic. Researchers all over the world have developed extensive studies through physical–chemical, biological techniques aiming to find a cost-effective process. However, conventional physical–chemical techniques such as adsorption on activated carbon, ultrafiltration, reverse osmosis, coagulation by chemical agents, and ion exchange on synthetic resins can only transfer organic compounds from one phase to another [3]. On the other hand, due to the large numbers of aromatic compounds present in dye molecules and the stability of modern dyes, traditional biological treatment by activated sludge is ineffective for decolourization and degradation [4,5].

In recent years, heterogeneous photocatalysis was proved to be an effective advanced oxidation technique for the complete decolourization of hazardous and refractory organic compounds, due to the high oxidation potential of active hydroxyl free radical (•OH) which is generated from irradiated semiconductor catalyst [6–10]. Among the various semiconductor catalysts employed, TiO_2 has been extensively studied because of its relative excellent properties such as high photosensitivity, strong oxidizing power under UV light irradiation, nontoxicity, long-term stability, and low cost. However, there are some drawbacks associated with its use: (i) electron–hole pairs recombination occurring within nanoseconds weakens the quantum effects [11]; (ii) the relatively large band gap (3.2 eV for anatase phase) does not allow the effective utilization of economical and ecological sunlight [12]. Due to these limitations, how to prepare the photocatalyst that can be excited by visible light and how to lengthen the electron–hole pairs recombination lifetime are of great interest for the development of photocatalytic process [13].

Cadmium sulfide (CdS) is a kind of semiconductor with narrow band gap of 2.5 eV, and its valence electron can be easily evoked to conduction band under visible light irradiation. Therefore, CdS semiconductor nanoparticles (NPs) have attracted intense interest due to their unique photochemical and photophysical properties. However, CdS NPs are easy to aggregate in aqueous solution and this metal sulfide is prone to photocorrosion. Biological synthesis of CdS NPs by yeasts and bacteria has been reported earlier in 1989 [14], and its photocatalytic activity has been verified [15,16]. The bioformation of CdS NPs is generally considered as the consequence of detoxification of intracellular Cd ions, and the binding

* Corresponding author at: No. 605, Dongfang Avenue, Linhai City, Zhejiang Province 317000, China. Tel.: +86 0139 8967 2070; fax: +86 0576 8513 7066.
E-mail addresses: jiangru0576@163.com (R. Jiang), zhuhuayue@126.com (H. Zhu), lxdfox@163.com (X. Li), xl9119@public.wh.hb.cn (L. Xiao).

1385-8947/$ – see front matter © 2009 Elsevier B.V. All rights reserved.
doi:10.1016/j.cej.2009.05.037

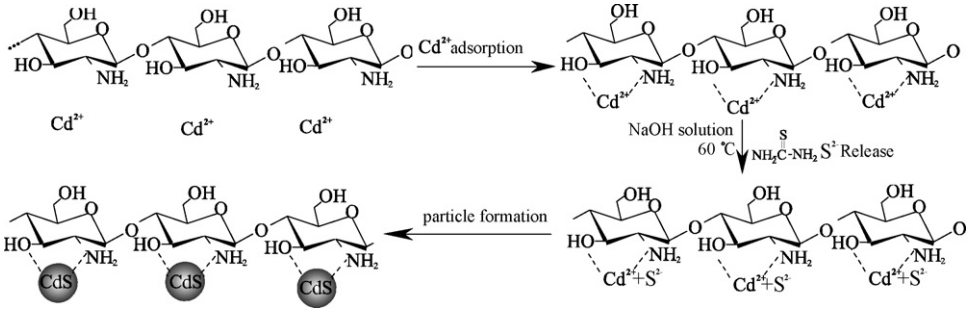

Fig. 1. Preparation mechanism of chitosan capped CdS nanoparticles.

of heavy metals by organisms through polysaccharide has also been demonstrated [17]. Furthermore, recent researches revealed that semiconductor sulfides could be utilized by some species in their energy circle, and in this process a polysaccharide layer was used to extract sulfur in the form of colloids [18]. These findings strongly suggest that polysaccharide plays an important role in the biosynthesis of CdS NPs. Thus, it is reasonable for us to design a polysaccharide-mediated route to mimic the biosynthesis of CdS NPs under relatively mild condition to control nanoparticles growth and minimize the electron–hole recombination.

Chitosan (CS) (1,4)-2-amino-2-deoxy-β-D-glucosamine, a natural basic, hydrophilic, nontoxic and biocompatible biopolymer obtained by the alkaline deacetylation of chitin [19], was reported to be the structural component of ascospore wall of yeast such as *Saccharomyces cerevisiae* [20]. Moreover, chitosan has good chelating ability with transition metal ions, which makes it possible for its metal ion complexes to be used as precursors to synthesize CdS NPs [21]. In addition, the amino and hydroxyl groups on linear chitosan chains are good capping groups for CdS NPs, and due to the highly viscous nature, chitosan can also prevent CdS NPs from agglomeration during the growth. Also, chitosan is a well-known excellent adsorbent for a number of organic dyes, which can further increase the photocatalytic decolourization of the composite catalyst.

However, there is few report on the effect of decolourization using chitosan capped CdS composite nanoparticles without loading TiO_2 for the photodegradation of dyes under visible light irradiation as far as we know. In this paper, we employed chitosan as capping material to biomimetically synthesize CdS NPs, i.e. CS/CdS NPs, under mild condition, and its photocatalytic activity was examined through C. I. Acid Red 66 (AR 66) photocatalytic decolourization under visible light irradiation. Parameters affecting the photocatalytic decolourization process, such as photocatalyst amount, solution pH, initial AR 66 concentration and photocatalyst reuse, have been investigated.

2. Experimental

2.1. Materials

The dye, C. I. Acid Red 66 (i.e. Biebrich Scarlet Red, $C_{22}H_{14}N_4Na_2O_7S_2$) was provided by China National Medicine Group Shanghai Chemical Reagent Company and used as received without further purification. Chitosan (CS, degree of deacetylation: 91.7%, Mw = 21×10^4) was purchased from Zhejiang Yuhuan Jinke Biochemisty Industry Co., Ltd. (Zhejiang, China). Other chemicals used in the experiments, cadmium chloride ($CdCl_2$, Shanghai Tianlian Fine Chemical Industry Co., Ltd., China), sulfocarbamide ($(NH_2)_2CS$, Shanghai Chemical Reagent Factory, China), 25% (v/v) glutaraldehyde (Shanghai Tianlian Fine Chemical Industry Co., Ltd., China) were of analytical grade. All the dye solutions were prepared by dissolving requisite quantity of dye in double distilled water.

2.2. Preparation of CS/CdS NPs composite catalyst

The synthetic procedure of CdS nanoparticles capped with chitosan was modified from previous literature report [22]. The preparation mechanism of chitosan capped CdS NPs is shown in Fig. 1. At room temperature, 1.5 g chitosan was dissolved in dilute nitric acid (100 mL, 1%, v/v) and stirring for 2 h. Then 0.9134 g $CdCl_2$ dissolved in 20 mL water was added into chitosan colloidal solution and continuously stirred for 4 h to reach a chelating balance. Subsequently, the colloidal mixture was dropped slowly into equimolar amounts sulfocarbamide aqueous solution in a constant temperature water bath at 60 °C for 1 h. The cross-linking agent glutaraldehyde (100 mL, 0.25%) was added to the mixed solution and stirred for 30 min. Finally, sodium hydroxide (200 mL, 0.1 mol/L) aqueous solution was introduced to precipitate chitosan capped CdS NPs. The golden yellow deposition was filtered and washed with distilled water and absolute ethyl alcohol for 3–4 times, and dried at 60 °C under atmospheric condition.

2.3. Photocatalytic reaction

The photocatalytic oxidation was carried out using a cylindrical homemade organic glass reactor (80 mm diameter and 110 mm depth), in which the slurry was composed of dye solution and catalyst. The reactor vessel was laid on a thermostat magnetic stirrer (model 85-2, Gongyi Yuhua Instrument Co. Ltd., China) with constant stirred magnetically and aerated by a simple air pump. Initial pH of solution was adjusted using dilute sulfuric acid or sodium hydroxide, and monitored by a pH/conductivity meter (model 990, Jiangsu Electroanalytical Instrument Factory, China). A 300 W Xenon lamp (PLS-SXE300, Beijing Trusttech Co. Ltd., China) loaded with a UV-Cut filter was used as artificial solar light source which basically emits visible light at 400–780 nm. The light intensity was kept approximately constant at 2 W/cm^2 10 cm away from the light source. At given irradiation time intervals, 4 mL of the suspensions were collected, then centrifuged and filtered through a Millipore filter (pore size, 0.22 in.) to separate the photocatalyst particles. The Millipore filter was washed using double distilled water every time to ensure that no residual dye and catalyst remained on the microfilter. AR 66 concentration was measured by Cary 50 Model UV–vis spectrophotometer (Varian, USA) scanning from 200 to 600 nm controlled by a Lenovo PC. All of the experiments were conducted at constant temperature 25 °C.

2.4. Characterization and analysis methods

The X-ray diffraction (XRD) spectra of chitosan and CS/CdS NPs were performed using a D8 ADVANCE X-ray diffraction spectrometer (Bruker, German) with a Cu Kα target at 40 kV and 50 mA at a scan rate of 0.02° $2\theta\,s^{-1}$.

The morphological structure of photocatalyst was examined by scanning electron microscopy (SEM) with a Hitachi SX-650 (Tokyo, Japan) machine.

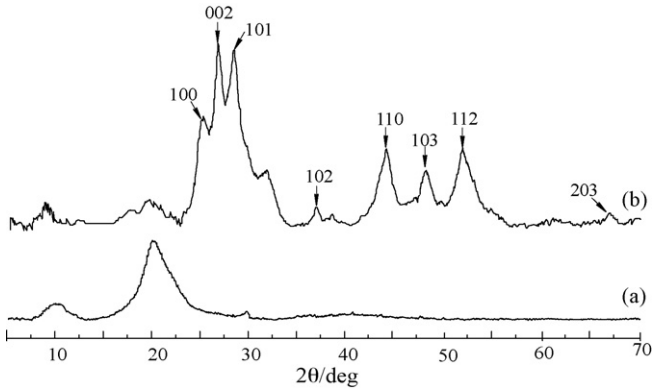

Fig. 2. XRD patterns of chitosan (a) and CS/CdS nanoparticles (b).

The TEM micrographs were taken using a transmittance electron microscope (TEM) [JEM-2010 FEF (UHR), JEOL, Japan] at an accelerating voltage of 200 kV.

Thermogravimetry (TG) was performed using a Setaram Setsys 16 TG/DTA/DSC (France) under a nitrogen atmosphere of 0.15 MPa from 25 to 800 °C with heating rate of 2 °C/min.

Photocatalytic activity of samples was assessed by decolourization rate. The percentage of decolourization (R) was estimated by the following:

$$R(\%) = \left(1 - \frac{C_i}{C_0}\right) \times 100 \quad (1)$$

where C_i was AR 66 concentration in aqueous solution at time T (mg/L); C_0 was initial AR 66 concentration (mg/L). Both were calculated by the standard curve equation for the wavelength of maximum absorbance (λ_{max} = 507.1 nm).

Several research results have indicated that the photocatalytic decolourization of various dyes fitted the Langmuir–Hinshelwood (L–H) kinetics model [23–26], which is commonly expressed:

$$-\frac{dC}{dt} = \frac{kKC}{1 + KC} \quad (2)$$

where k is the reaction rate constant (mg/L min); K is the adsorption coefficient of the reactant (L/mg); and C is the reactant concentration (mg/L).

When the concentration C is very small, KC is negligible with respect to unity, and the photocatalysis can be simplified to an apparent pseudo-first-order kinetics [23]:

$$-\frac{dC}{dt} = kKC \quad (3)$$

$$\text{i.e. } \ln\left(\frac{C_0}{C_i}\right) = kKt = k_{app}t \quad (4)$$

where k_{app} is the apparent pseudo-first-order rate constant (min^{-1}).

3. Results and discussion

3.1. X-ray diffraction (XRD)

X-ray power diffraction analysis method was employed to investigate the formation of chitosan capped CdS NPs (Fig. 2). The XRD pattern of chitosan (trace a) showed two typical peaks at 2θ = 11.8° and 20.9° [27], while the XRD pattern of chitosan capped CdS NPs (trace b) gave relatively weaken peaks. Other major diffraction peaks corresponded to the hexagonal phase according to Luan's report [28], which revealed the successful formation of hexagonal phase of CdS on chitosan by biomimetic synthesis method. The average size of the crystalline structure of the chitosan capped CdS NPs composite calculated by analysis of XRD data of (1 1 0), (1 0 2) and (1 0 3) was approximately 27 nm according to the Scherrer formula [29].

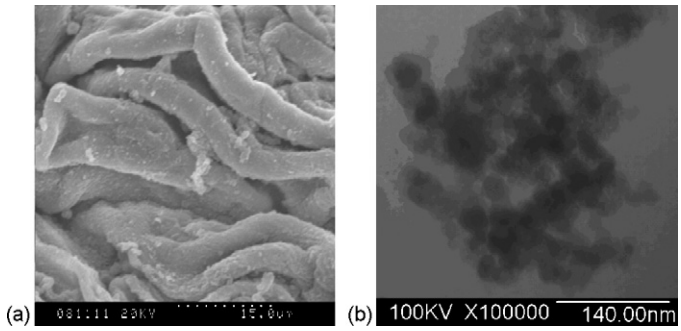

Fig. 3. SEM (a) and TEM (b) of representative chitosan capped CdS nanoparticles.

3.2. SEM and TEM

The direct evidence of the formation of nanoparticles on the surface of chitosan was given by SEM (Fig. 3a) and TEM (Fig. 3b). In Fig. 3a, there existed many pleats on the surface of chitosan capped CdS nanoparticles, which could provide a much larger surface area for photocatalytic reaction and adsorption process. Most of the particles embedded into chitosan had about diameters of 25–35 nm in the TEM image (Fig. 3b), which was in close agreement with XRD result.

3.3. TGA analysis

Fig. 4 presented the results of the DSC–TG analysis of the CS/CdS NPs composite catalyst. Three stages of weight loss were observed from the TG curve (trace a): (1) about 8% weight loss from room temperature to 131 °C, (2) 38% weight loss from 250 to 500 °C, and (3) 11% weight loss from 500 to 800 °C. The first stage of weight loss referred to the evaporation of physically adsorbed water [30]. Other stages of weight loss were due to the chemisorbed water and residual organics in the photocatalyst [19]. The total weight loss of CS/CdS NPs by 800 °C was about 7% more than that of cross-linked chitosan films, and the excess residual components were mostly CdS. It could be concluded that CS/CdS NPs composite exhibited better thermal stability than the pure chitosan.

3.4. Adsorption in dark and photocatalysis of AR 66 on CS/CdS NPs

As the photocatalytic mechanism suggests, both catalyst and a light source are necessary for the photocatalysis reaction to occur.

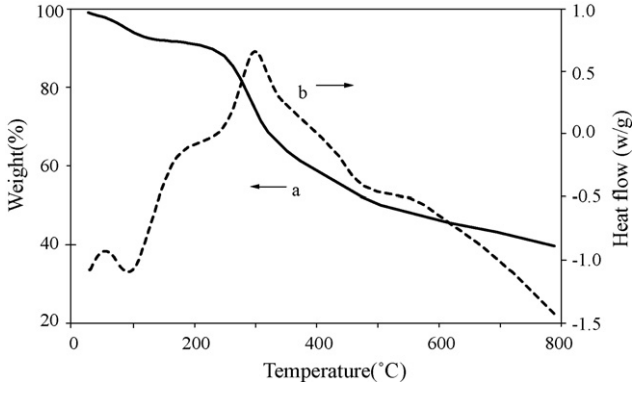

Fig. 4. TG (a) and DSC (b) analysis of representative chitosan capped CdS.

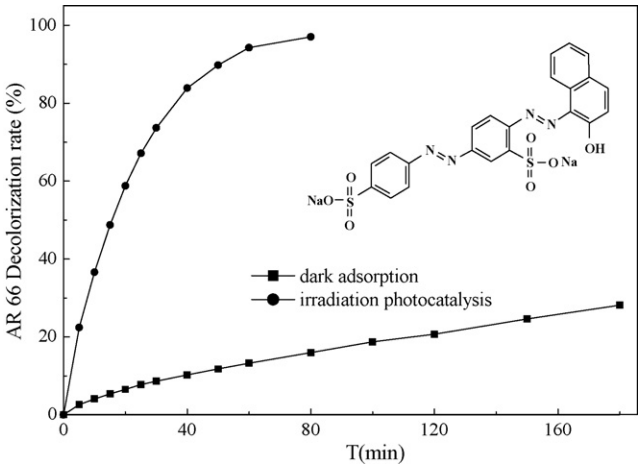

Fig. 5. Photocatalytic decolourization of AR 66 dye only in the presence of CS/CdS (0.7 g/L) adsorption in dark and in the presence of CS/CdS (0.7 g/L) under visible light irradiation. Inset: the chemical structure of AR 66.

A control experiment was conducted on the irradiation of AR 66 (20 mg/L) under only visible light, in the presence of CS/CdS NPs (0.7 g/L) with and without light irradiation, as shown in Fig. 5. Almost no decolourization was observed in the presence of visible light only. In the presence of CS/CdS NPs, without irradiation, only 13.3% was observed due to the adsorption of the dye within 60 min. It may be explained that a majority of $-NH_2$ and –OH groups, the main adsorbent groups in the chitosan, were cross-linked during synthesis of the composite. However, in the presence of CS/CdS NPs with visible light irradiation, about 36.6% and 94.3% were degraded after 10 and 60 min, respectively, as shown in Fig. 5, which indicated that the CS/CdS NPs had high photocatalytic activity. The photocatalysis and adsorption had synergistic effect for the dye colour removal.

3.5. Effect of the initial dye concentration

The effect of different initial dye concentrations on photocatalytic decolourization was investigated in the presence of 0.7 g/L catalyst at a normal pH of 5.6, as shown in Fig. 6. The percentage of decolourization decreased with the increased of the initial AR 66 dye concentration. The results were in good agreement with those reported in literatures [31,32]. The decolourization rates of dye were 90.5%, 73.6% and 37.3%, respectively, at the dye initial concentration

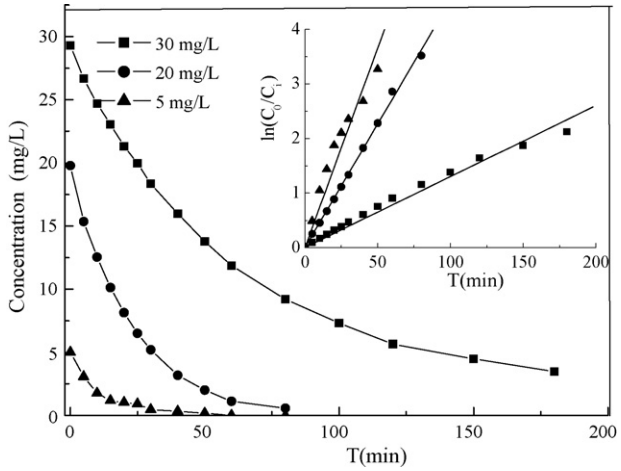

Fig. 6. Effect of initial dye concentration on AR 66 decolourization (pH 5.6, catalyst amount of 0.7 g/L). Inset: plot of $\ln(C_0/C_i)$ versus irradiation time.

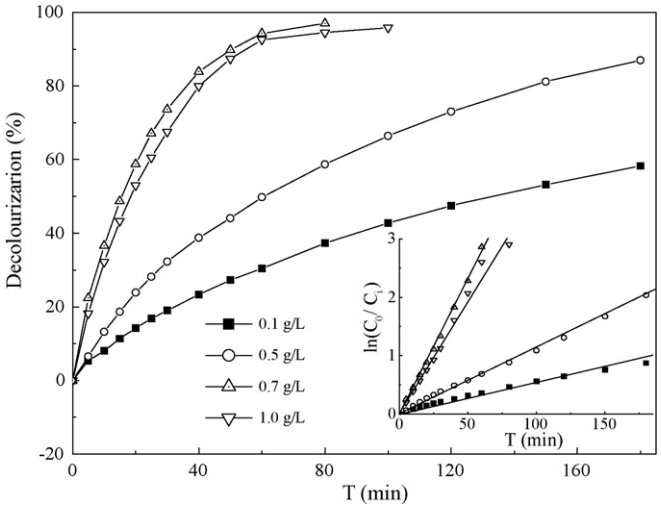

Fig. 7. Effect of catalyst amount on AR 66 decolourization (pH 5.6, $[AR]_0$ of 20 mg/L). Inset: plot of $\ln(C_0/C_i)$ versus irradiation time.

of 5, 20 and 30 mg/L after 30 min irradiation. The reason was that a high initial dye concentration shielded the light, which resulted in the decrease of the light triggered catalyst, thus the concentration of hydroxyl radicals decreased.

A plot of $\ln(C_0/C_i)$ versus irradiation time for different initial concentration of AR 66 is also shown in Fig. 6. The influence of initial concentration of the dye can be described by apparent pseudo-first-order kinetics in terms of the L–H model. Values of k_{app} can be obtained directly from the regression analysis of the linear curve in the plot. The reaction rate constants for 5, 20 and 30 mg/L were 0.07140, 0.04528 and 0.01301 min^{-1}, respectively.

3.6. Effect of catalyst amount

Photocatalyst amount is one of critical parameters to decolourization efficiency. In order to determine the effect of catalyst amount on decolourization of AR 66 and gain the optimum amount of CS/CdS NPs, a series of experiments were conducted with varying catalyst amount from 0.1 to 1.0 g/L, at dye concentration of 20 mg/L and pH 5.6. The effect of different catalyst amount on decolourization of AR 66 was shown in Fig. 7. The increase of catalyst amount from 0.1 to 0.7 g/L increased the dye decolourization sharply from 30.4% to 94.3% after 60 min irradiation. The decolourization of pollutants is influenced by the active site and the photo-absorption of the catalyst used. This was due to the increase in the catalyst amount, which contributed to the increase in the number of photons absorbed and also the number of dye molecule adsorbed [24,31]. But the increase in the catalyst amount beyond 0.7 g/L did not have an obvious positive effect on decolourization of AR 66 because of the enhancement of light reflectance and light blocking by excessive catalyst and decrease in light penetration. Accordingly, hydroxyl radicals, the primary oxidant in photocatalytic reaction, decreased and the decolourization efficiency of AR 66 reduced. The apparent rate constants of different catalyst amounts could be obtained from the plot of $\ln(C_0/C_i)$ versus irradiation time inserted in Fig. 7. It can be clearly seen that the 0.7 g/L catalyst amount had the highest photocatalytic decolourization of 0.04528 min^{-1} with correlation coefficient of 0.99865. Therefore 0.7 g/L was used as the optimal catalyst amount for photocatalytic reaction.

3.7. Effect of pH

Bahnemann et al. [34] have already reviewed that acid–base properties of the metal oxide surfaces can have considerable impli-

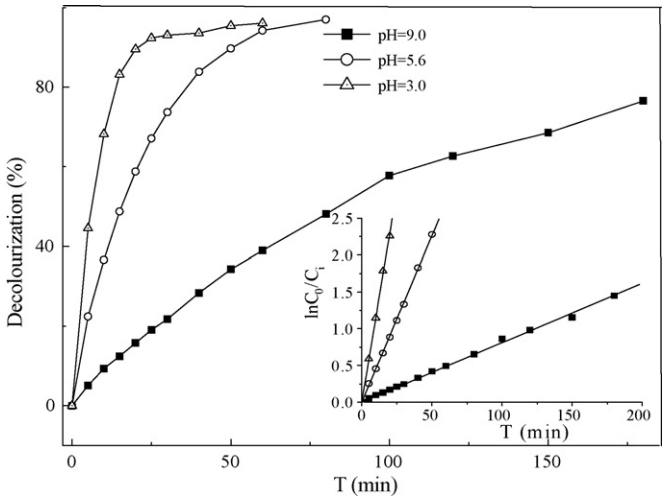

Fig. 8. Effect of initial pH on AR 66 decolourization ($[AR]_0$ of 20 mg/L, catalyst amount of 0.7 g/L). Inset: plot of $\ln(C_0/C_i)$ versus irradiation time.

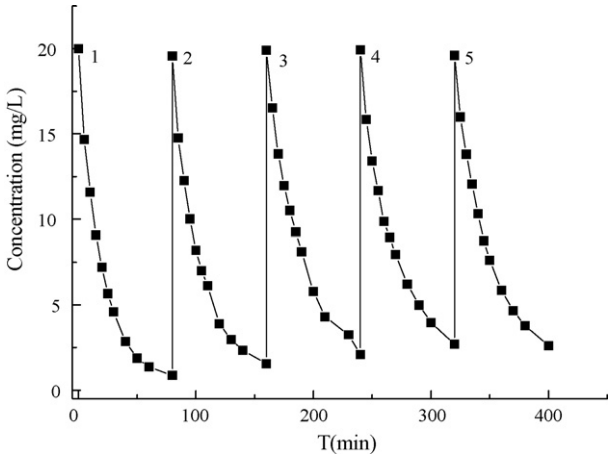

Fig. 9. The decrease of AR 66 concentration with visible light irradiation by recycling use of CS/CdS NPs (pH 5.6, catalyst amount of 0.7 g/L, $[AR]_0$ of 20 mg/L).

cations upon their photocatalytic activity. In order to investigate the effect of initial pH on photocatalytic decolourization of AR 66, three experiments were conducted at different pH values of 3.0, 5.6 and 9.0, at the initial dye concentration of 20 mg/L and the catalyst amount of 0.7 g/L. The results were illustrated in Fig. 8. Increase in the pH of AR 66 solution from 3.0 to 5.6 led to mildly decreased efficiency in the decolourization of AR 66. Further increase in pH from 5.6 to 9.0 had apparent decrease in AR 66 decolourization. After 60 min of irradiation, the calculated decolourization rate was 96.1% in the acidic medium (pH 3.0), 94.3% in the weak acidic medium (pH 5.6), and 38.9% in the alkaline medium (pH 9.0). The results indicated that the photocatalytic decolourization of AR 66 was most efficient in acidic solution than in alkaline solution.

The linear fit between the $\ln(C_0/C_i)$ and irradiation time for different initial pH of AR 66 solution can be approximated as pseudo-first-order kinetics, as shown in Fig. 8 (inset). The values of rate constants k_{app} and correlation coefficient R of decolourization process can be obtained directly from the straight line. The order of rate constants was pH 3.0 ($0.10967\,min^{-1}$) > pH 5.6 ($0.04528\,min^{-1}$) > pH 9.0 ($0.00834\,min^{-1}$). Correspondingly, the reaction half time for pH 3.0, 5.6 and 9.0 were 6.32, 15.31 and 83.11 min, respectively. This was because AR 66 molecule with two sulfuric groups ionized easily even in acidic media and became a soluble AR 66 anion. At the same time, the residual amino groups of chitosan in CS/CdS were much more easily to be protonated at lower pH and could form electrostatic attraction to adsorb a quantity of dye anions [33]. Therefore, in the acidic solution, AR 66 anions were easily adsorbed to CS/CdS with positive surface charge, while AR 66 anions were generally excluded away from surface of catalyst at alkaline media. The AR 66 anions could be oxidized more directly by hydroxyl radicals produced under visible light excitation in acidic media. That was why higher decolourization rates were obtained in acidic media. The possible photocatalytic decolourization mechanism of CS/CdS NPs in acidic solution may be expressed as follows:

(1) the first step is mainly the adsorption of azo anions on chitosan:

$$R_1\text{–}NH_3^+ + R_2\text{–}SO_3^- = R_1\text{–}NH_3^+ \bullet O_3S\text{–}R_2;$$

where R_1–NH_3^+ is chitosan, and R_2–SO_3^- is dye anions.

(2) the second step is photocatalytic decolourization of AR 66 on CS/CdS NPs:

$$CdS + h\nu \rightarrow CdS(h^+) + CdS(e^-)$$

$$CdS(h^+) + H_2O \rightarrow CdS + {}^\bullet OH + H^+$$

$${}^\bullet OH + RH \rightarrow \text{decolourization product}$$

3.8. Recycle of the catalyst

The catalyst's lifetime is an important parameter of the photocatalytic process, due to the fact that a longer period of time leads to a significant cost reduction of the treatment [35]. It is essential to evaluate the stability and reuse of the catalyst for practical implication. The photocatalytic experiments were repeated 5 times with the same catalyst at 20 mg/L dye concentration in the presence of 0.7 g/L catalyst at a normal pH of 5.6. After each experiment, the catalyst was centrifuged for 15 min, washed and recycled. The results showed that the catalytic activity of the catalyst had a slight decrease after 5 cycles and the results were shown in Fig. 9. The decolourization for the 5 cycling reuse were 93.1%, 88.1%, 83.7%, 80.7% and 80.1%, respectively, after 60 min of irradiation time. It showed a relatively small drop in decolourization efficiency, which was likely due to the loss of the catalyst during washing and filtrating. In spite of this, it could be concluded that the CS/CdS composite catalyst has relatively long using life.

3.9. UV–vis spectrum scan

Fig. 10 showed the obvious changes in the absorbance spectra ($200\,nm \le \lambda \le 600\,nm$) of AR 66 with CS/CdS NPs photocatalysis at different time intervals under visible light irradiation. The primary absorption peaks of the original dye solution were 507.1, 352, and 275 nm in the range of 200–600 nm. The absorbance at the maximum absorption peak (507.1 nm) corresponded to the $n \rightarrow \pi^*$ transition of the azo and hydrazone forms, which is due to the colour of azo dyes. The absorbance at 200–400 nm was attributed to the $n \rightarrow \pi^*$ transition of benzene rings, representing the aromatic content of azo dyes, and its decrease was due to the deconstruction of aromatic part of the dye [36,37]. As the reaction time increased, three peaks decreased gradually and the full spectrum scanning pattern changed obviously after 60 min. No peak was detected in

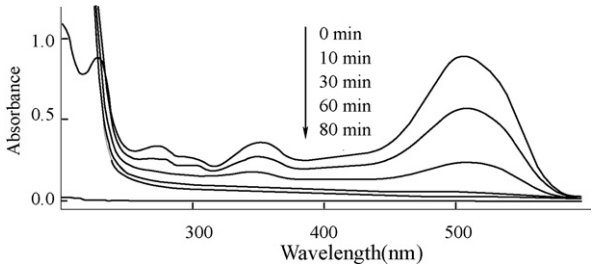

Fig. 10. Changes in UV–vis absorbance spectra of AR 66 with CS/CdS NPs at different time intervals under visible light irradiation.

the analyzed wavelength range at the end of the 80 min of reaction time. It indicated that the main chromophores and aromatic part in the original dye solution were destroyed in the presence of CS/CdS NPs under simulated solar light irradiation. UV–vis spectra were analyzed to indicate that the dye can be decoloured effectively by CS/CdS under visible light irradiation.

4. Conclusions

In the paper, chitosan was used as capping material to mimic the biosynthesis of CdS nanoparticles under relatively mild condition due to its metal sorption and chelation capability. CS/CdS NPs catalyst can be used effectively for AR 66 photocatalytic decolourization under visible light irradiation and oxygen supply. It is observed that the photocatalytic process followed apparent pseudo-first-order kinetics model. The decolourization was found to be relatively higher in the acidic medium with optimum catalyst amount of 0.7 g/L at low dye initial concentration. The recycle and reuse of catalyst was examined, and the results showed that the dye decolourization efficiency was still about 80.1% after 60 min of reaction time when catalyst was used for 5 times.

Acknowledgements

The authors are grateful for the financial support of this research from the National Natural Science Foundation of China (No. 50808071). Special thanks to Mr. Changhua Ge and Doctor Tang Lin for their assistance in this work.

References

[1] S.K. Kansa, M. Singh, D. Sud, Studies on photodegradation of two commercial dyes in aqueous phase using different photocatalysts, J. Hazard. Mater. 141 (3) (2007) 581–590.
[2] W.G. Kuo, Decolorizing dye wastewater with Fenton's reagent, Water Res. 26 (1992) 881–886.
[3] I.K. Konstantinou, T.A. Albanis, TiO_2-assisted photocatalytic degradation of azo dyes in aqueous solution: kinetic and mechanistic investigations., Appl. Catal. B: Environ. 49 (2004) 1–14.
[4] H. An, Q. Yi, X.S. Gu, W.Z. Tang, Biological treatment of dye wastewaters using an anaerobic-oxic system, Chemosphere 33 (1996) 2533–2542.
[5] Y. Li, D.L. Xi, Decolourization and biodegradation of dye wastewaters by a facultative-aerobic process, Environ. Sci. Pollut. Res. Int. 11 (2004) 372–377.
[6] A. Sobczyńsk, L. Duczmal, A. Dobosz, Photocatalysis by illuminated titania: oxidation of hydroquinone and *p*-benzoquinone, Monatsh. Chem. 130 (1999) 377–384.
[7] X. Li, W. Zhao, J. Zhao, Visible light-sensitized semiconductor photocatalytic degradation of 2,4-dichlorophenol, Sci. China Ser. B 45 (4) (2002) 421–425.
[8] E. Vulliet, C. Emmelin, J.M. Chovelon, C. Guillard, J.M. Herrmann, Photocatalytic degradation of the herbicide cinosulfuron in aqueous TiO_2 suspension, Environ. Chem. Lett. 1 (2003) 62–67.
[9] J.M. Herrmann, Heterogeneous photocatalysis: state of the art and present applications, Top. Catal. 34 (1–4) (2005) 49–65.
[10] J. Zhao, C. Chen, W. Ma, Photocatalytic degradation of organic pollutants under visible light irradiation, Top. Catal. 35 (3–4) (2005) 269–278.
[11] N. Serpone, E. Pelizzetti, Photocatalysis: Fundamentals and Applications, Wiley, New York, 1989, p. 342.
[12] S. Sakthivel, S.U. Geissen, D.W. Bahnemann, et al., Enhancement of photocatalytic activity by semiconductor heterojunctions: (-Fe_2O_3, WO_3 and CdS deposited on ZnO, J. Photochem. Photobiol. A: Chem. 148 (2002) 283–293.
[13] C.T. Juliana, M. Fabiano, C. Paola, et al., Electronic characterization and photocatalytic properties of CdS/TiO_2 semiconductor composite, J. Photochem. Photobiol. A: Chem. 181 (2006) 152–157.
[14] C.T. Dameron, R.N. Reese, R.K. Mehra, A.R. Kortan, P.J. Carroll, M.L. Steigerwald, L.E. Brus, D.R. Winge, Biosynthesis of cadmium sulphide quantum semiconductor crystallites, Nature 338 (1989) 596–597.
[15] W. Bae, R. Abdullah, R.K. Mehra, Cysteine-mediated synthesis of CdS bionanocrystallites, Chemosphere 37 (2) (1998) 363–385.
[16] P.R. Smith, J.D. Holmes, D.J. Richardson, D.A. Russel, J.R. Sodeau, Photophysical and photochemical characterization of bacterial semiconductor cadmium sulfide particles., J. Chem. Soc., Faraday Trans. 94 (9) (1998) 1235–1241.
[17] Z.A. Mohamed, Removal of cadmium and manganese by a non toxic strain of the fresh water cyanobacterium *Gloeothece magna*, Water Res. 35 (2001) 4405–4409.
[18] H. Tributsch, J.A. Chapana, Bioleaching of pyrite accelerated by cysteine, Process. Biochem. 45 (2000) 4705–4716.
[19] H. Yi, L.Q. Wu, W.E. Bentley, R. Ghodssi, G.W. Rubloff, J.N. Culver, G.F. Payne, Biofabrication with chitosan, Biomacromolecules 6 (2005) 2881–2894.
[20] P. Briza, A. Ellinger, G. Winkler, M. Breitenbach, Chemical composition of the yeast ascospore wall. The second outer layer consists of chitsan, J. Biol. Chem. 263 (1988) 11569–11574.
[21] B. Krajewska, Diffusion of metal ions through gel chitosan membranes, React. Funct. Polym. 47 (2001) 37–47.
[22] Z. Li, Y.M. Du, Z. Zhang, D.W. Pang, Preparation and characterization of CdS quantum dots chitosan biocomposite, React. Funct. Polym. 55 (2003) 35–43.
[23] Y. Li, X. Li, J. Li, J. Yin, Photocatalytic degradation of methyl orange by TiO_2-coated activated carbon and kinetic study, Water Res. 40 (2006) 1119–1126.
[24] J. Sun, X. Wang, J. Sun, R. Sun, S. Sun, L. Qiao, Photocatalytic degradation and kinetics of Orange G using nano-sized Sn(IV)/TiO_2/AC photocatalyst, J. Mol. Catal. A: Chem. 260 (2006) 241–246.
[25] X. Dong, W. Ding, X. Zhang, X. Liang, Mechanism and kinetics model of degradation of synthetic dyes by UV–vis/H_2O_2/Freeioxallate complexes, Dye Pigments 74 (2007) 470–476.
[26] C. Wu, H. Chang, J. Chen, Basic dye decomposition kinetics in a photocatalytic slurry reactor, J. Hazard. Mater. B 137 (2006) 336–343.
[27] R.J. Samuels, Solid State characterization of the structure of chitosan films, J. Polym. Sci. B: Polym. Phys. 19 (5) (1981) 1081–1105.
[28] Y.M. Luan, M.Z. An, M.R. Sun, Preparation and characterization of CdS/Cd nanoparticle film produced by electrodeposition, J. Chem. Eng. Chin. Univ. 18 (6) (2004) 745–750 (in Chinese).
[29] L. Wu, J.C. Yu, Fu X, Characterization and photocatalytic mechanism of nanosized CdS coupled TiO_2 nanocrystals under visible light irradiation, J. Mol. Catal. A: Chem. 244 (2006) 25–32.
[30] G.C. Ritthidej, P. Thawatchai, T. Koiaumi, Moist heat treatment on physicochemical change of chitosan salt films, Int. J. Pharm. 232 (2002) 11–22.
[31] S. Kaur, V. Singh, TiO_2 mediated photocatalytic degradation studies of Reactive red 198 by UV irradiation, J. Hazard. Mater. 141 (2007) 230–236.
[32] A.P. Toor, A. Verma, C.K. Jotshi, P.K. Bajpai, V. Singh, Photocatalytic degradation of direct yellow 12 dye using UV/TiO_2 in a shallow pong slurry reactor, Dyes Pigments 68 (2006) 53–60.
[33] H. Yoshida, A. Okamoto, T. Kataoka, Adsorption of acid dye on cross-linked chitosan fibers: equilibria, Chem. Eng. Sci. 48 (1993) 2267–2272.
[34] D.W. Bahnemann, J. Cunningham, M.A. Fox, E. Pelizzetti, P. Pichat, N. Serpone, in: R.G. Zeep, G.R. Helz, D.G. Crosby (Eds.), Aquatic Surface Photochemistry, Lewis Publishers, Boca Raton, 1994, p. 261.
[35] C. Wang, H. Shang, Y. Tao, T. Yuan, G. Zhang, Properties and morphology of CdS compounded TiO_2 visible-light photocatalytic nanofilms coated on glass surface, Sep. Purif. Technol. 32 (2003) 357–362.
[36] H. Park, W. Choi, Visible light and Fe(III)-mediated degradation of Acid Orange 7 in the absence of H_2O_2, J. Photochem. Photobiol. A 159 (2003) 241–247.
[37] M. Muruganandham, M. Swaminathan, Photochemical oxidation of reactive azo dye with UV/H_2O_2 process, Dyes Pigments 62 (2004) 269–275.